Quantum Chemical Designing of Efficient Sensitizers for Dye Sensitized Solar Cells

Muhammad Imran Abdullah, Muhammad Ramzan Saeed Ashraf Janjua,[†]
Asif Mahmood,[†,*] Sajid Ali,[‡] and Muhammad Ali[§]

Institute of Chemistry, University of the Punjab, Lahore, Pakistan
[†]Department of Chemistry, University of Sargodha, Sargodha, Pakistan. [*]E-mail: asifmahmood023@gmail.com
[‡]Department of Physics, Agriculture University, Faisalabad, Pakistan
[§]Department of Physics, Umea University, Umea, Sweden

Density functional theory (DFT) was used to determine the ground state geometries of indigo and new design dyes (IM-Dye-1 IM-Dye-2 and IM-Dye-3). The time dependant density functional theory (TDDFT) was used to calculate the excitation energies. All the calculations were performed in both gas and solvent phase. The LUMO energies of all the dyes were above the conduction band of TiO_2, while the HOMOs were below the redox couple (except IM-Dye-3). The HOMO-LUMO energy gaps of new design dyes were smaller as compared to indigo. All new design dyes were strongly red shifted as compared to indigo. The improved light harvesting efficiency (LHE) and free energy change of electron injection ΔG^{inject} of new designed sensitizers revealed that these materials would be excellent sensitizers. The broken coplanarity between the benzene near anchoring group having LUMO and the last benzene attached to TPA unit in all new design dyes consequently would hamper the recombination reaction. This theoretical designing will the pave way for experimentalists to synthesize the efficient sensitizers for solar cells.

Key Words : Dye-sensitized solar cells, Indigo, Light harvesting efficiency, Electron injection, Density functional theory

Introduction

Dye-sensitized solar cells (DSSC) attain consideration because of their sky-scraping light to electricity conversion efficiencies, simple and low cost manufacturing.[1-3] The sensitizer is a critical element in DSSC, which improves the power conversion efficiency and increases the stability of the devices. The Ruthenium base photosensitizers give a solar energy to electricity conversion efficiency of 10% in average.[2] Metal free organic DSSCs have benefits over metal holding sensitizers, *e.g.*, easy and cheap preparation methods, environment friendly and elevated molar extinction coefficient.[4] Different metal free dyes have been examined which have comparable efficiencies to metal holding sensitizers.[5-7] Designing of dye sensitizer plays an important role in the optimization of DSSC,[8] and it depends on the quantitative information of dye sensitizer.

In most of the organic sensitizers presence of donor, bridge and acceptor (DBA) moieties is very important to get better performance of the photoinduced intramolecular charge transfer. During electronic transition charge transfer depends on the conjugation across the donor and anchoring groups. Efficiency of organic sensitizers decreases due to dye aggregation and charge recombination.[9] It has been established that the triphenylamine (TPA)[10] derivatives as electron donor and cyanoacetic acid moiety as electron acceptor are better options to improve the efficiency.[9] It is estimated that TPA can restrain the cationic charge from the semiconductor surface therefore block the recombination. TPA also has a characteristics steric hindrance that can put off undesirable dye aggregation at the semiconductor surface.[11] To model and design efficient metal-free sensitizers for DSSC, suitable DBA systems are needed whose properties can be altered by applying the drivable structural modifications.

In this research work, we have studied the indigo and newly designed indigo base dyes. We have designed compounds by the substitution of TPA moiety in indigo dye as donor and cyanoacetic acid moiety, NO_2 and CN as electron acceptor. To evaluate the effect of auxillary donor on dye efficiency, Dimethyl Vinyl -$CH=C(CH_3)_2$ Methoxy and *N,N*-Dimethyl Amine groups have introduced on TPA moiety. This study will provide the help to experimentalists to synthesize the more efficient dyes for dye sensitized solar cells.

Computational Details

Density functional theory (DFT) and time dependant density functional theory (TD-DFT) calculations were performed to determine geometries, electronic structures and electronic absorption spectra of indigo base dyes. All the calculations, both in gas and solvent phase, were performed using Gaussian09 package.[12] All calculations were performed by employing CAM-B3LYP functional and 6-311+G* basis set. Polarizable continuum model (PCM) was used to study solvent effects.

The free energy change for electron injection onto a titanium dioxide (TiO_2) surface and dye's excited state oxidation potential were calculated using mathematical equations.

Following equation was used to calculate the free energy change for the process of electron injection.[13]

$$\Delta G^{inject} = E_{OX}^{dye*} - E_{CB}^{TiO_2} \tag{1}$$

E_{OX}^{dye*} is the excited state oxidation potential of the dye. $E_{CB}^{TiO_2}$ is the energy of conduction band of the TiO$_2$ semiconductor (−4.0 eV). E_{OX}^{dye*} was determined using following formula.

$$E_{OX}^{dye*} = E_{OX}^{dye} - \lambda_{max}^{ICT} \tag{2}$$

Where in this equation λ_{max}^{ICT} is the energy of intermolecular charge transfer (ICT). The light harvesting efficiency (LHE) was determined by formula[14]:

$$LHE = 1 - 10^{-f} \tag{3}$$

Where f is the oscillator strength of dye. TDDFT calculations provide the oscillator strength directly.

Results and Discussion

This study was carried out to design new sensitizers for DSSC application. The designed dyes consist of following parts: Auxiliary donor (AD), donor (D), pi-spacer (π) and acceptor (A) as shown in Figure 1. We have designed new dyes by the structural modification of indigo. Structure of indigo is given in Figure 2. In newly designed dyes, auxiliary donor and acceptors were changed. Structures of new design dyes are given in Figure 3. We have used CAM-
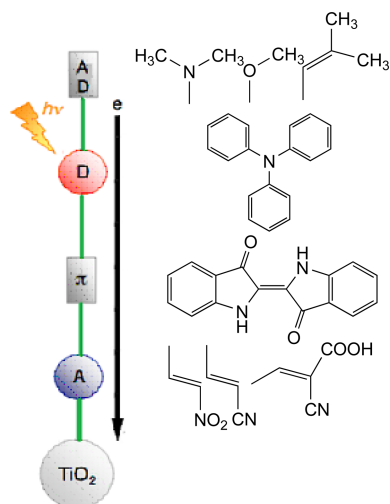

Figure 1. Different parts of AD-D-π-A system. AD = auxiliary donor, D = donor, π = pi-spacer, A = acceptor.
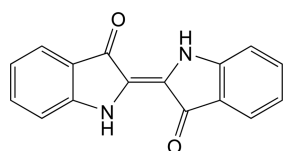

Figure 2. Chemical Structure of Indigo dye.

IM-Dye-1 R$_1$=R$_2$=CH=CH(CH$_3$), R$_3$=NO$_2$
IM-Dye-2 R$_1$=R$_2$=OCH3, R$_3$= CN
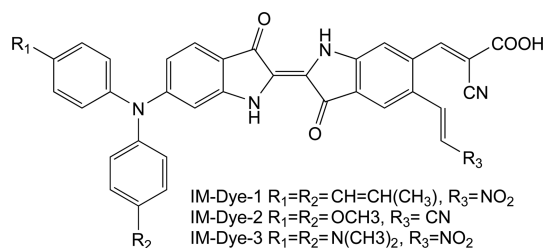IM-Dye-3 R$_1$=R$_2$=N(CH3)$_2$, R$_3$=NO$_2$

Figure 3. Chemical Structure of newly designed dyes.

B3LYP/6-311+G* for the optimization of indigo and three new designed sensitizers.

Electronic Structure. The distribution patterns of highest occupied molecular orbitals (HOMO) and lowest unoccupied molecular orbitals (LUMO) are used to study the efficiency of sensitizers. The distribution pattern of highest occupied molecular orbitals (HOMO) and lowest unoccupied molecular orbitals (LUMO) of new sensitizers are shown in Figure 4. From figure it is clear that HOMOs are present on TPA unit while LUMOs are present on benzene ring of the indigo near the anchoring group. Such electron density distributions are benecial for efcient charge separation and electron injection. This indicates the charge transfer from donor to acceptor through π-spacer. Significant charge transfer from donor to acceptor side proved that these dyes would be brilliant sensitizers. Highest occupied molecular orbitals energy (E$_{HOMO}$), lowest unoccupied molecular orbitals (E$_{LUMO}$) and HOMO-LUMO energy gap (E$_{gap}$) are given in Table 1.

The energy gaps of indigo and newly designed dyes in both gas phase and DMF are in following order IM-Dye-3 < IM-Dye-1 < IM-Dye-2 < indigo. This order can be explained on the basis of TPA moiety, nature of auxillary group on the TPA moiety and anchoring group (aceptor). Indigo has larger energy gap beacause it has no TPA moiety and anchoring group. Substitution of the electron donating groups at TPA benzene rings has enhanced the electron donating ability of TPA, while substitution of electron withdrawing groups at acceptor side has increased electron accepting ability of acceptor. In other words substitution of the electron donating groups at TPA benzene rings and withdrawing groups at acceptor side leads to efficient electron transfer, enhance the efficiency of dyes.

These dyes would be outstanding for DSSC as indicated by smaller HOMO-LUMO energy gaps of dyes in comparison to Indigo. HOMO of three new designed sensitizers delocalized over the pi-conjugated system with the greatest electronic cloud or density mostly at the central TPA-nitrogen atom, and the LUMO is positioned at acceptor side. It has been found that the HOMO-LUMO excitation stimulated by light irradiation might shift the electron distribution from the TPA-unit to the acceptor moiety and the photo-stimulated electron transfer from the dye to the TiO$_2$ electrode can take place powerfully by the HOMO-LUMO transition.

Spontaneous charge transfer from the dye excited state to conduction band of TiO$_2$ requires more positive potential LUMO energy than $E_{CB}^{TiO_2}$ (−4.0 eV), while spontaneous charge regeneration requires more negative HOMO energy
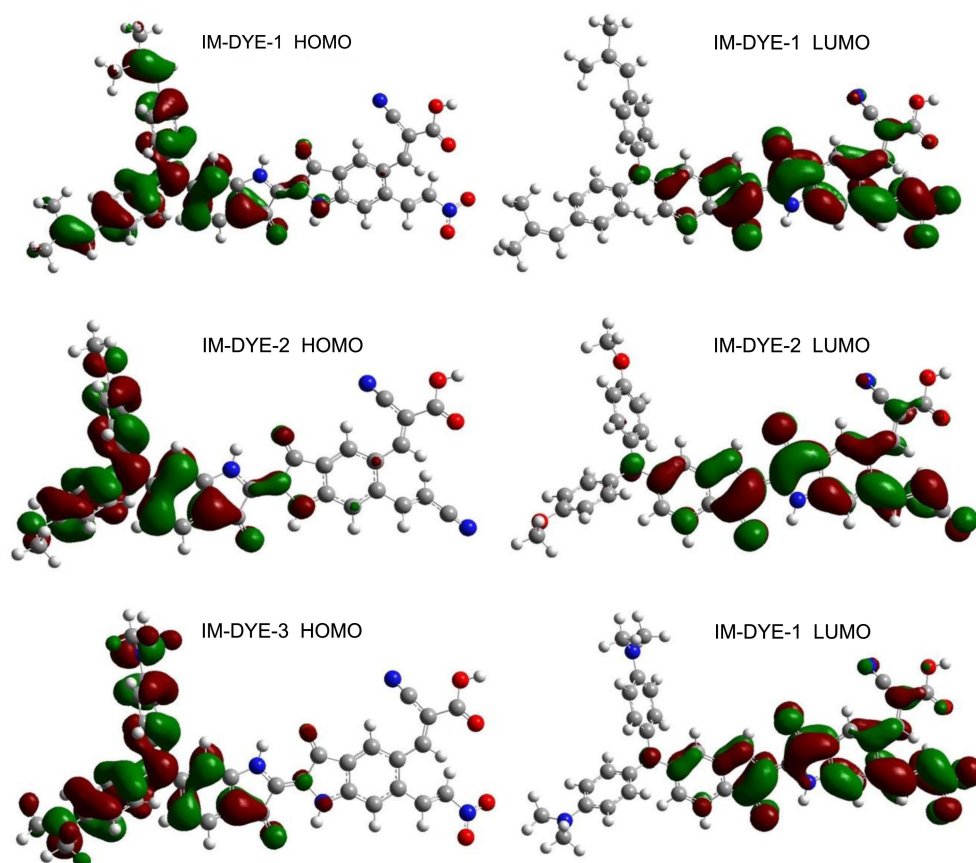
Figure 4. The HOMO and LUMO distribution pattern of dyes at DFT/CAM-B3LYP/6-311+G* level of theory.

Table 1. The E_{HOMO}, E_{LUMO} and energy gap (E_g) of dyes in eV at DFT/CAM-B3LYP/6-311+G* level of theory

System	Gas phase			DMF		
	E_{HOMO}	E_{LUMO}	E_{gap}	E_{HOMO}	E_{LUMO}	E_{gap}
Indigo	-5.2722	-2.7698	2.50	-5.3332	-2.8912	2.44
IM-Dye-1	-5.3859	-3.2926	2.09	-5.2270	-3.3170	1.90
IM-Dye-2	-5.4319	-3.0800	2.26	-5.2025	-3.0994	2.10
IM-Dye-3	-4.8896	-3.1285	1.76	-4.7525	-3.2667	1.48

Figure 5. Schematic energy diagram of dyes, TiO₂ and electrolyte (I⁻/I₃⁻). E_{HOMO} and E_{LUMO} of the dyes are in gas phase.

than reduction potential energy of the I^-/I_3^- electrolyte (−4.80 eV).[15] The energy level diagram of the HOMO and LUMO of the dyes, E_{cb} of TiO₂ and redox potential energy of the electrolyte are presented in Figures 5 and 6. Energies of HOMO and LUMO of the dyes were calculated in gas phase and DMF. The LUMOs of all dyes lies over the E_{cb} of TiO₂ while their HOMOs are lower than the redox potential energy of electrolyte (except IM-Dye-3). This indicates the spontaneous charge transfer and charge regeneration. From Figures 5 and 6 it is clear that indigo and new design dyes are good sensitizer.

Effect of Solvent on HOMO-LUMO Energies. The HOMO energy in DMF is greater than HOMO energy in gas phase. The LUMO energy in DMF is lesser than LUMO energy in gas phase. The DMF is an aportic polar solvent, it decreases the energy of LUMO and increases the energy of
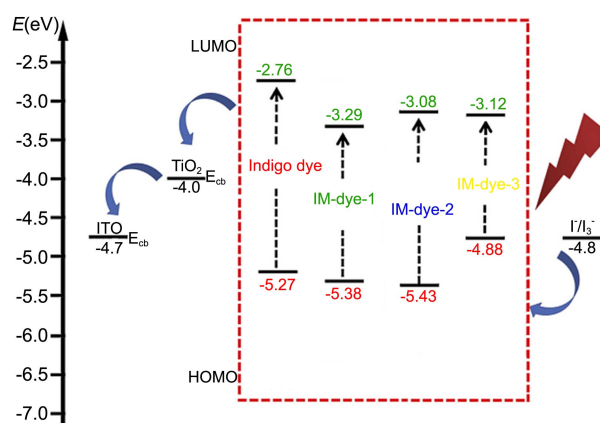
HOMO. Due these effects the energy gap becomes low in solvent phase as compared to gas phase, as shown in Table 1.

Free Energy Change of Electron Injection and Oxidation Potential Energy. We have used mathematical equations to estimate the dye's excited state oxidation potential and free energy change of electron injection to titanium dioxide (TiO₂) surface. λ_{max}, ΔG^{inject} λ_{max}^{ICT} E_{OX}^{dye} and E_{OX}^{dye*} are presented in Table 2. The electron injection free energy change ΔG^{inject}, ground and excited E_{OX}^{dye*} state oxidation potentials computed in gas phase and DMF. 6-311+G* basis set was
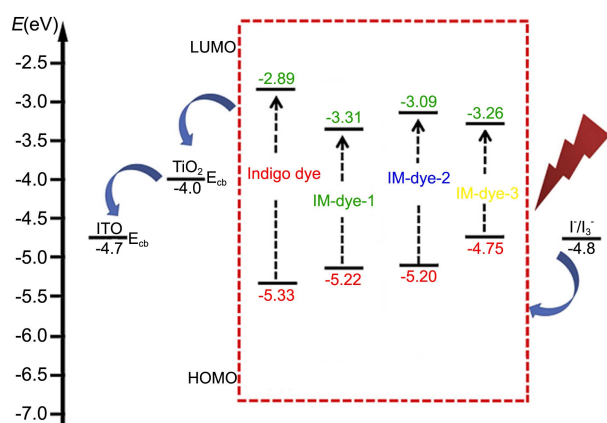
Figure 6. Schematic energy diagram of dyes, TiO$_2$ and electrolyte (I$^-$/I$_3^-$). E$_{HOMO}$ and E$_{LUMO}$ of the dyes are in DMF.

used for all calculations. E_{OX}^{dye} can be estimated as negative E$_{HOMO}$.[16] E_{OX}^{dye*} is calculated based on Eq. (2) ΔG^{inject} was estimated using Eq. (1). Its values are negative for all dyes. In parent molecule ΔG^{inject} is −1.0384 in gas phase while it is −0.8295 in DMF because of lowering of LUMO energy in solvent phase. In all new designed dyes IM-Dye-1, IM-Dye-2 and IM-Dye-3 ΔG^{inject} improved both in gas phase and solvent phase as shown in Table 2. The negative ΔG^{inject} is an indication of spontaneous electron injection from the dye to TiO$_2$. For all newly designed dyes ΔG^{inject} is more negative than indigo. Order of ΔG^{inject} is: IM-Dye-3 < IM-Dye-2 < IM-Dye-1 < indigo.

Light Harvesting Efficiency (LHE) and Oscillator Strength. The light harvesting efficiency (LHE) is the effi-

ciency of dye to response the light. It is another factor which indicates the efficiency of DSSC. The light harvesting efficiency (LHE) of the dye should be as high as feasible to maximize the photo-current response.

The oscillator strength is directly obtained from TDDFT calculations. The Indigo dye has two main absorption peaks (536 and 321 nm in gas phase, 584 and 333 nm in solvent phase DMF). Higher oscillator strength of three new designed sensitizers is due to better pi-conjugation. We have calculated the LHE of the main absorption peaks and then we have calculated the average LHE which is higher for the new designed sensitizers than indigo as shown in Table 3. These dyes will convert more light to electrical energy.

The oscillator strength and transition character are given in Table 4. Only the transitions with considerable oscillator strengths are given. The electronic structures of three new designed sensitizers are quite similar even though their substituent groups are dissimilar from one another. The HOMO and LUMO composition of new sensitizers are depicted in Figure 4. The electron distribution of the HOMO orbital is delocalized on the π-system with the maximum electron density present on the Benzene rings and nitrogen of TPA in all new designed sensitizers. It is noticed that the LUMO orbital have highest compositions on anchoring group and benzene ring of the acceptor side in all new designed sensitizers. Therefore, electron will move from donor to acceptor during the HOMO-LUMO excitation resulted by light absorption.

Improve ΔG^{inject} and LHE of new designed sensitizers as compare to indigo is due to the replacement of hydrogen of TPA at R$_1$ and R$_2$ position with Vinyl -CH=C(CH$_3$)$_2$,

Table 2. Calculated absorption spectra λ$_{max}$, ΔG^{inject}, oxidation potential, intramolecular charge transfer energy of dyes at TDDFT/CAM-B3LYP/6-311+G* level of theory

System	Gas phase					DMF				
	λ$_{max}$ nm	ΔG^{inject}	E_{OX}^{dye*}	E_{OX}^{dye}	λ_{max}^{ICT}	λ$_{max}$ nm	ΔG^{inject}	E_{OX}^{dye*}	E_{OX}^{dye}	λ_{max}^{ICT}
Indigo	536.5	-1.038	2.961	5.272	2.310	573.2	-0.829	3.170	5.333	2.162
IM-Dye-1	674.0	-0.453	3.546	5.385	1.839	750.6	-0.424	3.575	5.227	1.651
IM-Dye-2	623.4	-0.556	3.443	5.431	1.988	682.2	-0.614	3.385	5.202	1.817
IM-Dye-3	805.1	-0.650	3.349	4.889	1.539	976.7	-0.516	3.483	4.752	1.269

Table 3. Excitation energy (E), Light Harvesting Efficiency (LHE) and average Light Harvesting Efficiency (LHE$_{Average}$) of dyes at TDDFT/CAM-B3LYP/6-311+G* level of theory

System	Gas phase				DMF			
	E/eV	λ nm	LHE	LHE$_{Average}$	E/eV	λ nm	LHE	LHE$_{Average}$
Indigo	2.310	536.5	0.458	0.434	2.162	573.2	0.530	0.549
	3.858	321.3	0.410		3.749	330.6	0.568	
IM-Dye-1	1.839	674.0	0.509	0.505	1.651	750.5	0.597	0.613
	2.089	593.3	0.599		1.942	638.2	0.628	
IM-Dye-2	1.988	623.4	0.537	0.606	1.817	682.2	0.679	0.692
	2.215	559.7	0.675		2.104	589.0	0.705	
IM-Dye-3	1.539	805.1	0.404	0.510	1.269	976.7	0.498	0.541
	2.059	602.0	0.636		1.933	641.1	0.584	

Table 4. Oscillator strength (f) and Transition character of dyes (H = HOMO, L = LUMO, L+1 = LUMO+1, *etc.*) at TDDFT/CAM-B3LYP/ 6-311+G* level of theory

System	Gas phase			DMF		
	λ/nm	(f)	Transition character[a]	λ/nm	(f)	Transition character[a]
Indigo	536.5	0.266	H → L (100%)	573.2	0.328	H → L (100%)
	321.3	0.229	H-3 → L (91%)	330.6	0.364	H-3 → L (95%)
	273.6	0.169	H → L+2 (86%)	272.2	0.180	H → L+2 (91%)
IM-Dye-1	674.0	0.309	H → L (99%)	750.5	0.395	H → L (99%)
	593.3	0.397	H-1 → L (99%)	638.2	0.430	H-1 → L (99%)
	498.1	0.130	H → L+1 (97%)	547.7	0.161	H → L+1 (98%)
IM-Dye-2	623.4	0.335	H → L (98%)	682.2	0.494	H → L (99%)
	559.7	0.488	H-1 → L (98%)	589.0	0.530	H-1 → L (99%)
	469.8	0.013	H → L+1 (98%)	383.6	0.289	H-4 → L (90%)
IM-Dye-3	805.1	0.227	H → L (100%)	976.7	0.300	H → L (100%)
	602.0	0.416	H-1 → L (98%)	666.2	0.225	H → L+1 (94%)
	572.9	0.080	H → L+1 (99%)	454.6	0.247	H-2 → L+2 (91%)

[a]Major contribution to the transitions are in parenthesis.

-OCH$_3$ and -N(CH$_3$)$_2$ group on donor side and addition of -CH=CH-CN, -CH=CH-COOH and -CH=CH-NO$_2$ groups on acceptor side. This can also be confirmed by analyzing the distribution pattern of HOMO and LUMO of IM-Dye-1, IM-Dye-2 and IM-Dye-3. The comprehensive charge transfer has been observed from donor to acceptor moieties. The replacement of hydrogen of TPA at R$_1$ and R$_2$ position with Vinyl -CH=C(CH$_3$)$_2$, -OCH$_3$ and –N(CH$_3$)$_2$ group on donor side and addition of -CH=CH-CN, -CH=CH-COOH and -CH=CH-NO$_2$ groups on acceptor side encourages the promotion of the electron injection. The steric hindrance of the TPA prevents the dye aggregation and recombination.

Absorption Analysis. The molecular orbital of Indigo involved in transitions state were calculated by the TD-CAM-B3LYP/6-311+G* in Gas Phase and DMF. The calculated absorption spectrum (λ_{max}) of Indigo is 536 and 573 nm in gas phase and DMF respectively. Which is very close to the experimental λ_{max} of Indigo (540 and 600 nm in Gas phase and DMF respectively).[17,18] Comparison of calculated and experimental λ_{max} of Indigo show that CAM-B3LYP/6-311+G* is reliable approach to calculate the absorption spectrum (λ_{max}). Absorption spectrum (λ_{max}) of three new designed sensitizers was calculated using CAM-B3LYP/6-311+G* in Gas Phase and DMF.

UV-VIS absorption spectra of indigo, IM-Dye-1, IM-Dye-2 and IM-Dye-3 are shown in Figures 7 and 8. Both consist of a very intense and well separated absorption band in the 200-1350 nm region. The spectrum of Indigo is red-shifted in DMF. The spectrum of three new designed sensitizers IM-Dye-1, IM-Dye-2 and IM-Dye-3 in DMF (750 nm, 682.23 nm and 976.78 nm) is marvelously red-shifted in comparison with that of IM-Dye-1, IM-Dye-2 and IM-Dye-3 in gas phase (674.07, 623.43 and 805.19 nm respectively). Solvent effect on the absorption spectrum of indigo is less. λ_{max} changed from 536 to 573 nm. The overall spectral red-shift was in following order: IM-Dye-3 > IM-Dye-2 > IM-Dye-1 > indigo dye. This order is reverse to the order of HOMO-
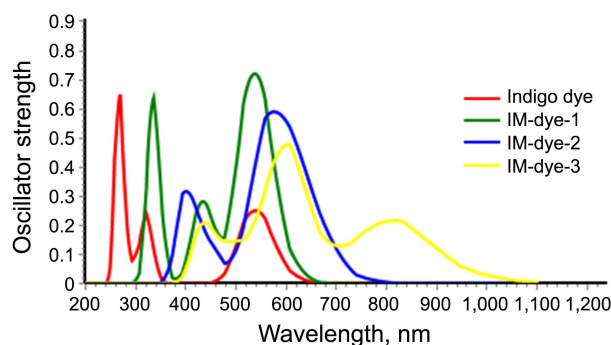

Figure 7. Simulated absorption spectra of dyes calculated in Gas Phase at TDDFT/CAM-B3LYP/6-311+G* level of theory.
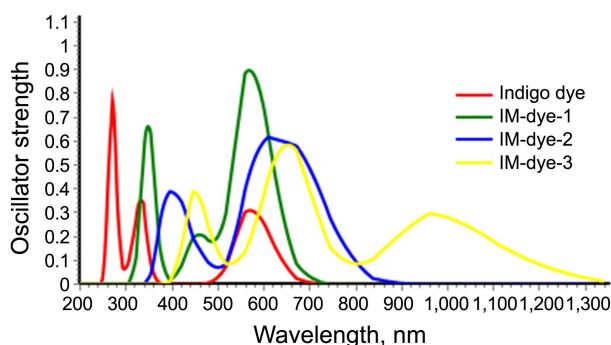

Figure 8. Simulated absorption Spectra of dyes calculated in DMF at TDDFT/CAM-B3LYP/6-311+G* level of theory.

LUMO energy gap. Dyes which have low energy gap require less energy for electronic transition. Low energy transitions result red shifted absorption wavelength.

The first absorption band belongs to the HOMO-LUMO transition, and is of ICT character thus having high transition intensity and low electron excitation energy. The second intense band also belongs to a π-π* transition.

The absorption spectrum of IM-Dye-3 shows that it absorbs in near infrared region as well as in visible region. It could

theoretically absorb from 400 nm to 1350 nm. So we can say that that dye will work in dim light by the absorption of infrared radiation. This dye is also environment friendly because it absorbs the infrared which cause global warming. On the other hand the IM-Dye-2 and IM-Dye-1 absorbs in visible region.

Conclusions

The HOMO is delocalized over the pi-conjugated systems with the highest electron density located at the central TPA-nitrogen atom, and the LUMO are located at the anchoring groups through the pi-bridge in all new designed dyes. The LUMO energies of all new designed dyes are above the conduction band of TiO_2, and HOMO energies below the redox couple (except IM-Dye-3). The computed λ_{max} of Indigo was 536 and 584 nm in gas phase and DMF respectively. Which are very close to the experimental values (540 nm and 600 nm in gas phase and respectively). All new designed dyes IM-Dye-1, IM-Dye-2 and IM-Dye-3 were highly red shifted as compared to Indigo due to solvent effect. The ΔG^{inject} and LHE of new designed photo-sensitizers were improved as compared to indigo. Electron donating groups on TPA side, electron withdrawing on acceptor side and indigo as a bridge promotes the electron injection and light harvesting efficiency. The steric hindrance of the TPA prevents the dye aggregation and recombination on semi-conductor surface.

References

1. Regan, B. O.; Gratzel, M. *Nature* **1991**, *353*, 737-740.
2. Nazeeruddin, M. K.; De Angelis, F.; Fantacci, S.; Selloni, A.; Viscardi, G.; Liska, P.; Ito, S.; Takeru, B.; Grätzel, M. *J. Am. Chem. Soc.* **2005**, *127*, 16835-16847.
3. Zhang, Q. F.; Dandeneau, C. S.; Zhou, X. Y.; Cao, G. Z. *Adv Mater* **2009**, *21*, 4087-4108.
4. Li, G.; Jiang, K. J.; Li, Y. F.; Li, S. L.; Yang, L. M. *J Phys Chem C* **2008**, *112*, 11591-11599.
5. Wong, B. M.; Codaro, J. G. *J. Chem. Phys.* **2008**, *129*, 214703-214710.
6. Horiuchi, T.; Miura, H.; Sumioka, K.; Uchida, S. *J. Am. Chem. Soc.* **2004**, *126*, 12218-12219.
7. Ferrere, S.; Zaban, A.; Gregg, B. *J. Phys. Chem. B* **1997**, *101*, 4490-4493.
8. Robertson, N. *Angew. Chem. Int. Ed.* **2006**, *45*, 2338-2345.
9. Liu, D.; Fessenden, R. W.; Hug, G. L.; Kamat, P. V. *J. Phys. Chem. B* **1997**, *101*, 2583-2590.
10. Hagfeldt, A.; Gratzel, M. *Acc. Chem. Res.* **2000**, *33*, 269-277.
11. Sayama, K.; Tsukagochi, S.; Hara, K.; Ohga, Y.; Shinpou, A.; Abe, Y.; Suga, S.; Arakawa, H. *J. Phys. Chem. B* **2002**, *106*, 1363-1371
12. Frisch, M. J. *et al.* Gaussian 09, Revision A.1. Gaussian Inc, Wallingford, CT, 2009.
13. Katoh, R.; Furube, A.; Yoshihara, T.; Hara, K.; Fujihashi, G.; Takano, S.; Murata, S.; Arakawa, H.; Tachiya, M. *J. Phys. Chem. B* **2004**, *108*, 4818-4822.
14. Nalwa, H. S. Handbook of advanced electronic and photonic materials and devices; Academic: San Diego, 2001.
15. Wichien, S.; Samarn, S.; Vittaya, A. *J. Photochem. Photobiol. A* **2012**, *236*, 35-40.
16. Preat, J.; Michaux, C.; Jacquemin, D.; Perpète, E. A. *J. Phys. Chem. C* **2009**, *113*, 16821-16833.
17. Tomkinson John, Bacci Mauro, Picollo Marcello, Colognesi Daniele. *Vib. Spectrosc.* **2009**, *50*, 268-276.
18. Zollinger, hristie, 2007 Methods of Determining Indigo: *Handbook of Natural Colorants* Edited by Thomas Bechtold and Rita Mussak©2009 John Wiley & Sons: Ltd., 2003; p 106-107.